Desalination and Water Treatment
www.deswater.com

doi: 10.5004/dwt.2019.24434

163 (2019) 190–197
September

Adsorption of chromium (VI) and phosphorous (V) from aqueous solution by calcined Mg–Al–CO_3 hydrotalcite-like compound

Xiaoliang Zhang*, Xuanmin Song

Institute of Mining Technology, Taiyuan University of Technology, Shanxi 030024, China, Tel. +86 18234085118; email: kv.zh.xl@gmail.com (X. Zhang), Tel. +86 15513629200; email: xuanmsong@163.com (X. Song)

Received 27 October 2018; Accepted 19 May 2019

ABSTRACT

Mg–Al–CO_3 hydrotalcite-like compound (HTlc) was synthesized by coprecipitation method, and HTlc was calcined under 500°C to obtain calcined Mg–Al–CO_3 hydrotalcite-like compound (CHTlc). The samples were examined by X-ray diffraction and Fourier transform infrared spectroscopy. Adsorption properties of chromium (VI) (Cr(VI)) and phosphorous (V) (P(V)) on CHTlc were investigated. A series of experiments were performed to study the influence of various experimental parameters, such as contact time, pH, initial concentration, and adsorbent dosage. Competitive adsorption characteristics of Cr(VI) and P(V) on CHTlc were investigated and the adsorbent regeneration experiment was carried out. Results indicate that the optimum adsorption could be achieved with 1 g L^{-1} adsorbent solution (20 mg L^{-1} Cr(VI) and 20 mg L^{-1} P(V)) at a pH of approximately 5 in 8 h. Cr(VI) adsorption in co-existing solution system of the two anions is obviously suppressed by P(V), while Cr(VI) had no significant influence on P(V) adsorption. The adsorbent can be regenerated within 10%Na_2CO_3 + 5%NaOH solution. After three regeneration cycles, the adsorption removal rate of Cr(VI) and P(V) had not changed significantly.

Keywords: Hydrotalcite-like compounds; Chromium (VI); Phosphorous (V); Water treatment

1. Introduction

Chromium is a common pollutant in water and soil, which typically occurs in two oxidation states in the natural environment, water treatment processes and water distribution systems: trivalent chromium (chromium-3, Cr(III), Cr^{+3}), and hexavalent chromium (chromium-6, Cr(VI), Cr^{+6}) [1]. Cr(VI) is generally present in surface and ground water. Various industries such as electroplating, metal cleaning, leather processing and mining discharge Cr(VI)-containing wastewater with various concentrations (5–220 mg L^{-1}) of Cr(VI) into the aquatic environment [2]. Cr(VI) is toxic and can cause various types of harm to people, such as skin allergies, hereditary gene deletion and carcinogenic [3,4]. Due to its strong oxidizability and high toxicity, Cr(VI) is always viewed as a carcinogen and mutagen [5,6]. Phosphorus is generally present in nature in the form of phosphate, and the +5 state (phosphorus (V), P(V)) for the element is its stable state. P(V) is an important factor of surface freshwater system, which can limit the growth of plants. However, excess P(V) can cause serious environmental problems in lakes and reservoirs, such as eutrophication, algae blooming, and ecosystem damage [7]. There are many sources of P(V) in water such as mineral processing, detergents, electronic industry, pigments, and over use of P(V)-containing fertilizer [8]. Moreover, excess P(V) can cause intense accumulation of algae, which may lead to decrease of aquatic life [9]. These pollutants can pollute soil, groundwater and other environmental system, ultimately threatening human health. Therefore, removal of Cr(VI) and P(V) from wastewater before discharging into the environment is significantly important.

---

* Corresponding author.

1944-3994/1944-3986

Various methods were employed by researchers for the removal of Cr(VI), such as chemical precipitation [10], chemical reduction [11,12], membrane separation [13,14], electrocoagulation [15,16], ion exchange [17,18], photocatalytic reduction [19,20], and adsorption [21–25]. For P(V) removal, chemical precipitation [26], microfiltration [27,28], crystallization [29–31] and adsorption [32–36] are extensively used.

P(V) and Cr(VI) often appear together in wastewater, such as wastewater from mineral processing. There are simultaneous removal techniques for Cr(VI) and P(V), such as hybrid anion exchange precipitation [37] and liquid–liquid extraction [38]. Among these techniques, adsorption is one of the most promising because of its efficiency, flexibility, and low cost.

Hydrotalcite-like compound material (HTlc) is a kind of layered compound composed of positively charged layers of metal sheets and negatively charged anions. The general chemical formula is $M^{2+}_{1-x}M^{3+}_{x}(OH)_2]^{x+}A^{m-}_{x/m}\cdot n\mathrm{H_2O}$, where M^{2+} is a divalent cation, M^{3+} is a trivalent cation, $x(= M^{2+}/M^{2+} + M^{3+})$ is the layer charge density, A^{m-} is an interlayer anion, and n is the number of interlayer water molecules. HTlc has special layered structure, large specific surface area, and adjustable anions between the layers. The anion exchange and memory effect of HTlc material are the main properties that enable this material to remove toxic anionic species from aqueous systems as a potential adsorbent [39–41]. HTlc affinities for anions generally follow the order of the Hofmeister series [42]. In other words, the affinity increases with the decrease of ionic radius and increase of charge. For monovalent inorganic anions, the affinity decreases in the order of $\mathrm{OH^-} > \mathrm{F^-} > \mathrm{Cl^-} > \mathrm{Br^-} > \mathrm{NO_3^-} > \mathrm{I^-}$. In addition, the affinity of HTlc for multivalent inorganic anions is generally greater than for monovalent inorganic anions. $\mathrm{CO_3^{2-}}$, which is generally the interlaminate anion, is preferentially adsorbed and inhibits further ion exchange [43]. The interlayer $\mathrm{CO_3^{2-}}$ anion can be removed by calcining at a certain temperature [44]. At a certain temperature, HTlc can exist in the form of bimetallic oxide after calcination (CHTlc). CHTlc can absorb water and anions to restore its original layered structure when placed in the air or in a solution containing certain anions, which is called the memory effect [45,46]. The adsorption capacity of CHTlc for removal of hazardous anions from contaminated water is better than HTlc because the calcination of HTlc containing $\mathrm{CO_3^{2-}}$ as interlayer anion causes the formation of $M^{2+}M^{3+}O$ solid solution capable of recovering the HTlc layered structure during the treatment of anions from aqueous solution. When CHTlc recover its original structure, anions compete to occupy the sites previously occupied by $\mathrm{CO_3^{2-}}$ in the lamellar structure, and there are some parameters influence this process. When CHTlc is used to remove fluoride from an aqueous solution, the adsorption process is influenced by pH, adsorbent concentration and temperature of aqueous solution. Various anions compete to be adsorbed onto CHTlc in the order $\mathrm{PO_4^{3-}} > \mathrm{Cl^-} \approx \mathrm{SO_4^{2-}} > \mathrm{Br^-} > \mathrm{NO_3^-}$ when fluoride aqueous solution contains other anions. The Z/r (charge/radius) values of the anions vary in the order $\mathrm{PO_4^{3-}}$ (3/3.40) > $\mathrm{SO_4^{2-}}$ (2/2.40) > $\mathrm{Cl^-}$ (1/1.81) > $\mathrm{Br^-}$ (1/1.95) > $\mathrm{NO_3^-}$ (1/2.81), that is, CHTlc may have a greater affinity for anions with higher charge densities [47]. For removal of Cr(VI) and phosphate by CHTlc, phosphate showed a stronger affinity for CHTlc compared with that manifested by Cr(VI), and the factors influencing this affinity include contact time, solution pH, and initial anion concentrations [48]. Moreover, HTlc is easy to synthesize, inexpensive and reusable. Thus, HTlc is considered to be one of the most promising inorganic functional materials [49]. Because of these features, CHTlc is used in this paper as an adsorbent to remove Cr(VI) and P(V) from aqueous solution and further be used in wastewater treatment.

This paper aims to study the adsorption of Cr(VI) and P(V) under different conditions, which may provide guidance for practical engineering applications. Aqueous solution was prepared to simulate wastewater, and CHTlc was used as adsorbent. In order to effectively utilize CHTlc, several factors were analyzed separately, such as time, pH, initial concentration and adsorbent dosage. Moreover, the mutual influence between Cr(VI) and P(V) and the regenerative properties were studied. Finally, recycling of the materials was considered to further reduce operation costs.

2. Experimental

2.1. Sample preparation and characterization

The CHTlc used in this experiment was prepared by a liquid-phase co-precipitation method. Solution A was prepared by dissolving 25.6 g $\mathrm{Mg(NO_3)_2\cdot 6H_2O}$ and 18.75 g $\mathrm{Al(NO_3)_3\cdot 9H_2O}$ in deionized water. NaOH (20 g) was dissolved in deionized water to make solution B.

Solution A and solution B were added to a $\mathrm{Na_2CO_3}$ solution at a rate of 1 drop per second under constant stirring, and the pH of mixed solution was maintained at approximately 11 with $\mathrm{HNO_3}$ and NaOH. The mixture was stirred for 30 min after adding solution A and solution B. Then the mixture was placed in a constant 65°C water bath for 18 h. The final precipitate was filtered, washed thoroughly, and dried at 80°C for 12 h to obtain $\mathrm{Mg{-}Al{-}CO_3}$ HTlc. Calcined $\mathrm{Mg{-}Al{-}CO_3}$ HTlc was obtained by calcining the $\mathrm{Mg{-}Al{-}CO_3}$ HTlc at 500°C for 5 h.

X-ray diffraction (XRD) and Fourier transform infrared (FTIR) spectroscopy were used to examine the CHTlc samples. XRD patterns were obtained in a Rigaku D/Max-2500 diffractometer (Rigaku, Tokyo, Japan) with CuKα radiation (voltage 40 kV, current 30 mA, scan rate 8°min^{-1}, scanning range from 5° to 65°). FTIR spectra of KBr pellets were recorded on a Thermo-Nicolet Nexus 670 FTIR spectrometer (Thermo Nicolet, Madison, WI, USA) (wavenumber range from 400 to 4,000 cm^{-1}).

2.2. Adsorption experiments

Cr(VI) and P(V) solution were prepared, respectively, with dissolving $\mathrm{K_2Cr_2O_7}$ and $\mathrm{KH_2PO_4}$ in deionized water. The pH value of samples during the experiment was adjusted with 0.2 mol L^{-1} $\mathrm{HNO_3}$ and 0.2 mol L^{-1} NaOH. A 30.0°C ± 0.2°C constant temperature shaker was used in experiments at a rotational speed of 150 rpm.

Water samples were filtered for analysis of the concentrations of residual Cr(VI) and P(V) solution. The concentration of Cr(VI) before and after sorption processes was determined by diphenyl carbazide method, with spectrophotometer

(721 model spectrophotometer, Shanghai Third Analytical Instrument Factory, Shanghai, China) at a wavelength of 540 nm. And the concentration of P(V) before and after sorption processes was identified by molybdate blue method, colorimetric reading of a spectrophotometer (721 model spectrophotometer, Shanghai Third Analytical Instrument Factory, Shanghai, China) at a wavelength of 700 nm.

The adsorption capacity q_t (mg g^{-1}) at specific time t was determined by Eq. (1):

$$q_t = \frac{\left(C_0 - C_t\right)V}{1,000W} \tag{1}$$

The removal rate R_t (%) at specific time t was calculated by the following Eq. (2):

$$R_t = \frac{\left(C_0 - C_t\right)V}{C_0 V} \times 100\% \tag{2}$$

where C_0 (mg L^{-1}) is the initial Cr(VI) or P(V) concentration, C_t (mg L^{-1}) is the Cr(VI) or P(V) concentration at specific time t, V (L) is the solution volume, and W (mg) is the adsorbent mass.

The equilibrium adsorption capacity q_e (mg g^{-1}) and the equilibrium removal rate R_e (%) could be calculated by Eqs. (1) and (2), respectively, where C_t at equilibrium was replaced by C_e (equilibrium Cr(VI) or P(V) concentration, mg L^{-1}).

2.2.1. Effect of adsorption time

A Cr(VI) and P(V) mixed sample (200 mL) was prepared in which both Cr(VI) and P(V) had initial concentration of 20 mg L^{-1}. Then, 0.1 g CHTlc was added, and the mixture was stirred in a thermostatic shaker. The concentrations of Cr(VI) and P(V) were measured at specific times (0.25, 0.5, 1, 1.5, 2, 3, 4, 5, 6, 8 and 11 h).

2.2.2. Effect of pH in experiments

Five identical mixed samples (5 × 200 mL) containing Cr(VI) (20 mg L^{-1}) and P(V) (20 mg L^{-1}) were prepared. The pH of the five samples was, respectively, adjusted to 3, 5, 7, 9, and 11 with 0.2 mol L^{-1} HNO_3 and 0.2 mol L^{-1} NaOH. Then, adsorbent (5 × 0.1 g) was added to the samples. The samples were placed in a thermostatic shaker for 8 h. Then, the pH, Cr(VI) concentration, and P(V) concentration were measured.

2.2.3. Effect of initial Cr(VI) and P(V) concentration in experiments

Five samples (5 × 200 mL) containing the same Cr(VI) concentration (20 mg L^{-1}) but different P(V) concentrations (0, 5, 10, 20, 30, and 40 mg L^{-1}) were prepared. Then, added CHTlc (5 × 0.1 g) to every sample, and the mixed solution samples were placed in a thermostatic shaker for 8 h. The concentration of Cr(VI) in every sample was measured.

The other group of five samples (5 × 200 mL) containing the same P(V) concentration (20 mg L^{-1}) but various Cr(VI) concentrations (0, 5, 10, 20, 30, and 40 mg L^{-1}) were prepared. Added CHTlc (5 × 0.1 g) to every sample, the mixed solution samples were placed in thermostatic shaker for 8 h. The concentration of P(V) in every sample was measured.

2.2.4. Effect of dosage in experiments

Identical samples (6 × 200 mL) containing Cr(VI) (20 mg L^{-1}) and P(V) (20 mg L^{-1}) were prepared, and the pH value of samples was adjusted between 5 and 6. Then different amounts of CHTlc were added, respectively, to six samples, to final CHTlc concentrations of 0.5, 0.6, 0.7, 0.8, 0.9, and 1.0 g L^{-1}. The six samples were placed in a thermostatic shaker for 8 h. The concentrations of Cr(VI) and P(V) in every sample solution were measured.

2.3. Recycle method

A sample solution (200 mL) containing Cr(VI) (20 mg L^{-1}) and P(V) (20 mg L^{-1}) was prepared. CHTlc (0.2 g) was added to the sample solution. Then, the mixed solution sample was placed in a thermostatic shaker for 8 h. CHTlc-500 (containing Cr(VI) and P(V)) was obtained after the mixed solution was filtered and dried. The CHTlc-500 (containing Cr(VI) and P(V)) was added to 200 mL Na_2CO_3 (10%) and NaOH (5%) mixed solution and stirred for 8 h. Then, the mixture was filtrated and dried. Regenerated CHTlc was obtained by calcining the precipitate at 500°C for 5 h.

Regenerated CHTlc-500 (containing Cr(VI) and P(V)) was used as adsorbent, and the experiment was repeated three times under the same conditions.

3. Results and discussion

3.1. Sample characterization

The XRD patterns of Mg–Al–CO_3 HTlc and CHTlc-500 are shown in Fig. 1. The HTlc XRD patterns demonstrated the characteristic peaks of hydrotalcite-like compounds (e.g., 003, 006, and 009) [50]. The strong X-ray reflection proved a high degree of crystallinity and a layered structure in the samples. The diffraction peaks disappeared after calcining at 500°C, indicating that the hydrotalcite-like structure had collapsed and that the stacking of the layers became disordered [34]. The broad peaks shown in the figure were caused by the formation of Mg–Al mixed oxides.

The peak shape is sharp and symmetric, which proves that the obtained hydrotalcite has high crystallinity and good regularity. In the CHTlc-500 pattern, the characteristic hydrotalcite diffraction peaks have disappeared, indicating that the original layered structure was destroyed and converted to double metal oxide.

The FTIR spectra of Mg–Al–CO_3 HTlc and CHTlc-500 are shown in Fig. 2. The band at 3,434 cm^{-1} corresponds to the stretching vibration of O–H bonds in metal hydroxides and water molecules. The band at 1,627 cm^{-1} is attributed to the bending vibration of water molecules between the layers. In addition the band at 1,360 cm^{-1} corresponds to the characteristic vibration of CO_3^{2-} [51]. The bands at 400–1,000 cm^{-1} are produced by infrared adsorption of interlayer anions and metal-hydrogen bonds. As seen by comparing the infrared spectra of HTlc and CHTlc-500, the bands at 1,627 and 1,360 cm^{-1} decreased significantly, which proves that

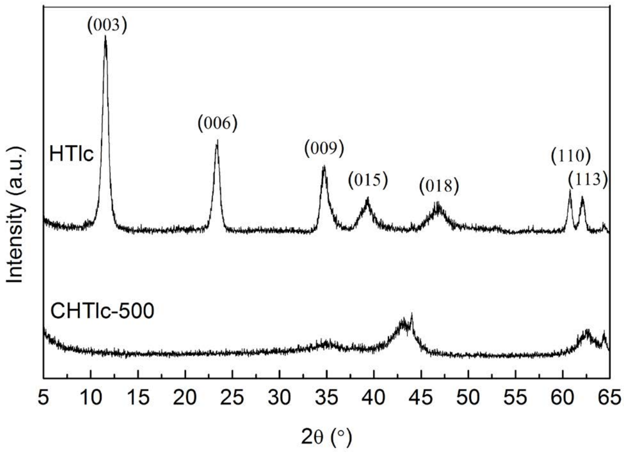

Fig. 1. XRD spectra of HTlc and CHTlc-500.

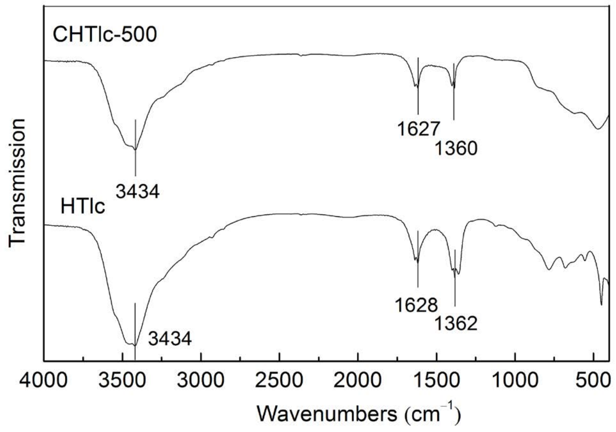

Fig. 2. FTIR spectra of HTlc and CHTlc-500.

most CO_3^{2-} and water molecules between HTlc laminates were lost after calcination. The results also demonstrated that CO_3^{2-} was not completely removed after calcining at 500°C and that there was a strong affinity between CO_3^{2-} and HTlc.

3.2. Effect of time factor

To determine the equilibration time, the time required for Cr(VI) and P(V) to be adsorbed by CHTlc-500 was investigated. The relationship between adsorption time and the amount of Cr(VI) and P(V) adsorbed by CHTlc-500 is shown in Fig. 3. The amounts of Cr(VI) and P(V) adsorbed on CHTlc-500 both initially increased with time and steadily reached equilibrium. The adsorption of P(V) is faster than that of Cr(VI) and gradually increased with time. By approximately 5 h, the adsorption of P(V) reached equilibrium, and the equilibrium amount of P(V) adsorbed on CHTlc-500 was 40 mg g^{-1}. The amount of Cr(V) adsorbed on CHTlc-500 increased slowly from 0 to 5 h. Then increased quickly after 5 h, and reached equilibrium at approximately 8 h with a total amount adsorbed of 18.12 mg g^{-1}. Considering that equilibrium was reached in less than 8 h, the equilibration time for subsequent experiments was set to 8 h. The amount of P(V) adsorbed onto CHTlc-500 is more than that of Cr(VI), and P(V) reached equilibrium faster than Cr(VI). This difference may be because Cr(VI) and P(V) compete for the same adsorption sites, and the affinity of P(V) on CHTlc-500 is greater than that of Cr(VI).

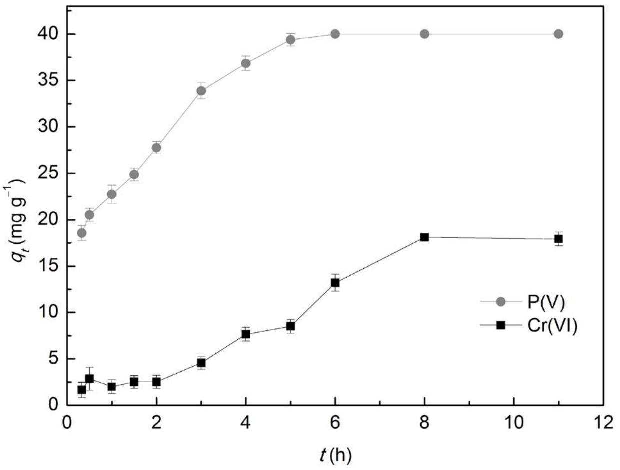

Fig. 3. Effect of time on Cr(VI) and P(V) adsorption by CHTlc-500.

3.3. Effect of pH

Solution pH is an important factor affecting adsorption because it controls the surface change of adsorbent and the speciation of ions. Fig. 4 shows the adsorption of P(V) and Cr(VI) on CHTlc-500 at different initial pH values with a constant ionic density. When the solution pH increased from 3 to 5, the adsorption capacity of Cr(VI) and P(V) increased. Both Cr(VI) and P(V) reached maximum adsorption when the pH was approximately 5. As the pH varied from 7 to 11, the adsorption of Cr(VI) and P(V) clearly decreased. Therefore, a pH of approximately 5 was considered to be favorable for the adsorption process.

According to previous research, when the pH of a solution is less than 5, a large amount eluted metal ions can be detected in solution [52]. Although the released Al^{3+} experiences a flocculation effect, the performance of CHTlc-500 under such

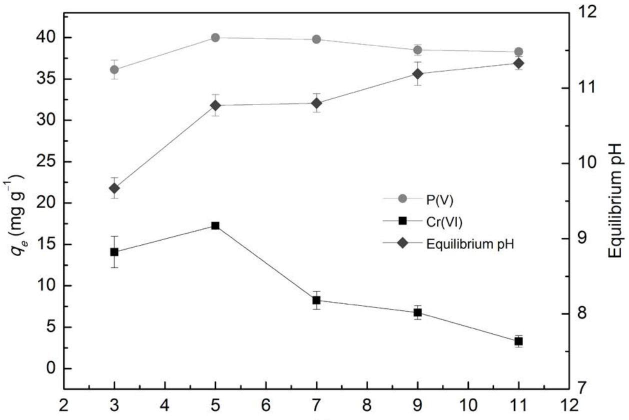

Fig. 4. Effect of initial pH value on Cr(VI) and P(V) adsorption by CHTlc-500.

conditions is instable, which may explain why the adsorption capacity of Cr(VI) and P(V) at pH less than 5 was low.

Similarly, a peralkaline environment is not conducive to CHTlc-500 adsorption. With increasing pH, the excess OH^- in solution competes with the adsorbate for adsorption sites, and the OH^- attached to the CHTlc-500 surface exerts an electrostatic repulsion effect on other ions.

The results could be due to the excess OH^-, which can compete with Cr(VI) and P(V) for sites on the lamellar structure during the adsorption process. In addition, a higher pH can promote the formation of negative ions, which would inhibit the adsorption of ions [53].

Additionally, when the initial pH increased from 7 to 11, the amount of adsorbed Cr(VI) and P(V) decreased:

$$HCrO_4^- \Leftrightarrow CrO_4^{2-} + H^+ \quad pK = 5.9 \tag{3}$$

$$H_2PO_4^- \Leftrightarrow HPO_4^{2-} + H^+ \quad pK = 7.2 \tag{4}$$

It can be inferred from Eqs. (3) and (4) that more adsorption will need to occur to adsorb the same amount of contaminants when the anions in solution are converted from monovalent to divalent ions, which means that CHTlc-500 adsorbs 2 mol $H_2PO_4^-$ or $HCrO_4^-$ equals to adsorb 1 mol HPO_4^{2-} or CrO_4^{2-}. Thus, when the pH was high, the adsorption of Cr(VI) and P(V) was reduced.

Fig. 4 shows that the Cr(VI) adsorption process is more apt to be affected by pH than the adsorption of P(V). P(V) was able to interact with CHTlc much more easily than Cr(VI) did, because the affinity between P(V) and CHTlc is stronger than that between CHTlc and Cr(VI).

CHTlc has some buffering effect on the pH of the solution [54,55]. In Fig. 4, when the initial pH of the mixture ranges from 3 to 11, the balanced mixture pH generally increased in the range from 9 to 12. After Cr(VI) and P are adsorbed on CHTlc-500, the solution becomes alkaline, which is related to the reaction mechanism by which inorganic anions X^{m-} rebuild their original layered structure [56].

$$m\mathrm{Mg}_{1-x}\mathrm{Al}_x\mathrm{O}_{1+\frac{x}{2}} + x\mathrm{X}^{m-} + \left(m+n+\frac{mx}{2}\right)\mathrm{H_2O} \rightarrow \left[\mathrm{Mg}_{1-x}\mathrm{Al}_x(\mathrm{OH})_2\right]_m (X)_x \times n\mathrm{H_2O} + mx\mathrm{OH}^- \tag{5}$$

Eq. (5) shows that OH^- is released during the process of CHTlc-500 adsorption of Cr(VI) and P(V), thus increasing acidity of the system. Considering this process, CHTlc-500 may also be applied for neutralization of certain inorganic acid wastewater, thus reducing the cost of pH adjustment treatments.

3.4. Competition between Cr(VI) and P(V) in adsorption system

In Fig. 5, the Cr(VI) curve represents how the initial P(V) concentration (increased from 0 to 40 mg L^{-1}) impacts the adsorption of Cr(VI), and the P(V) curve shows how the initial Cr(VI) concentration (increased from 0 to 40 mg L^{-1}) impacts the adsorption of P(V). As the curves show, the change in the Cr(VI) concentration had little effect on P(V) adsorption, and the removal rate of P(V) remains above 99%. The removal rate of Cr(VI) was high when the concentration of P(V) increased from 0 to 10 mg L^{-1}. However, when the concentration of P(V) increased from 10 to 20 mg L^{-1}, the removal rate of Cr(VI) decreased significantly from 98.17% to 43.14%. As the concentration of P(V) increased from 20 to 40 mg L^{-1}, the removal rate of Cr(VI) continued decreasing but decreased at a lower rate. Such phenomena suggest that Cr(VI) and P(V) compete for adsorption sites on CHTlc-500, with a certain CHTlc-500, P(V) is more apt to occupy adsorption sites because of its stronger affinity. In the first group, the P(V) concentration was 20 mg L^{-1}, but the Cr(VI) concentration varied from 0 to 40 mg L^{-1}. During the adsorption process, it was difficult for Cr(VI) to compete with P(V) for adsorption sites on CHTlc-500. Thus, the effect of Cr(VI) for the adsorption of P(V) on CHTlc-500 was small. In the other group, the Cr(VI) concentration was 20 mg L^{-1} but the P(V) concentration varied from 0 to 40 mg L^{-1}. When the P(V) concentration varied from 0 to 10 mg L^{-1}, there were enough adsorption sites on CHTlc-500 for both Cr(VI) and P(V), so the impact of P(V) on Cr(VI) was small. For a certain amount of CHTlc-500, when the P(V) concentration increased, Cr(VI) and P(V) competed for adsorption sites on CHTlc-500. P(V) is more apt to occupy adsorption sites, so the amount of Cr(V) adsorbed on CHTlc-500 became less; thus, the removal rate of Cr(VI) decreased. Consequently, there was less CHTlc-500 surface area available for Cr(VI), and the Cr(VI) adsorption capacity decreased [57]. There are two main reasons that explain the adsorption capacity difference between Cr(VI) and P(V). The first reason is that the ionic radius of phosphate is smaller than that of chromate, so it is easier for phosphate ion to occupy adsorption sites between CHTlc-500 laminates. Moreover, the configuration and electrical properties of the structures composed of Cr(VI) and P(V) differ from each other.

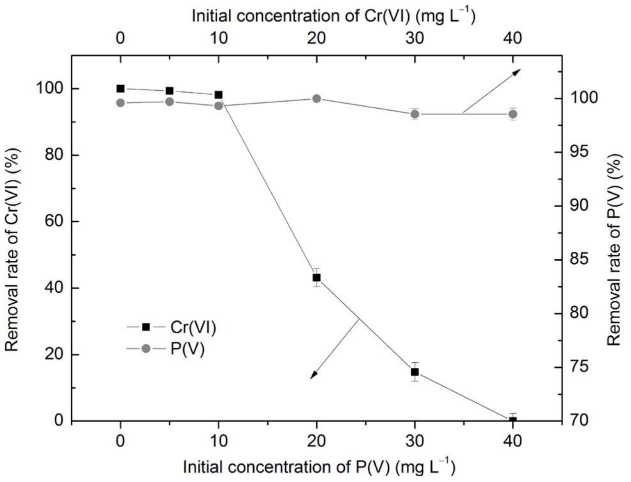

Fig. 5. Mutual effects of Cr(VI) and P(V) with different initial concentration.

3.5. Effect of adsorbent dosage

Because Cr(VI) and P(V) occupy the same adsorption sites on CHTlc-500, increasing the adsorbent dosage means more adsorption sites are available for both Cr(VI) and P(V). Table 1 lists the adsorption equilibrium concentrations of

Table 1
Effect of CHTlc-500 dosage on Cr(VI) and P(V) adsorption

Dosage (g L^{-1})	Cr(VI) equilibrium concentration (mg L^{-1})	P(V) equilibrium concentration (mg L^{-1})
0.5	11.372	0.003
0.6	4.754	0
0.7	2.267	0
0.8	0.106	0
0.9	0.068	0
1.0	0	0

Cr(VI) and P(V) under different CHTlc-500 dosage. The initial concentrations of Cr(VI) and P(V) were 20 mg L^{-1}, and when the CHTlc-500 dosage was 0.5 g L^{-1}, the equilibrium removal rates of Cr(VI) and P(V) were 43.14% and 99.99%. When the CHTlc-500 dosage increased to 0.6 g L^{-1}, the equilibrium removal rates of Cr(VI) and P(V) were 76.23% and 100%. Upon increasing the CHTlc-500 dosage, the Cr(VI) removal rate increased rapidly. When the dosage reached 1.0 g L^{-1}, both Cr(VI) and P(V) had been fully processed. A possible explanation for this finding was that the number of adsorption sites for Cr(VI) and P(V) on CHTlc-500 increased as CHTlc-500 dosage increased. Cr(VI) and P(V) compete for adsorption sites on CHTlc-500 when the concentration of CHTlc-500 is not sufficient. P(V) is more apt to occupy adsorption sites than Cr(VI), so the removal rate of P(V) is larger than that of Cr(VI). When the dosage of CHTlc-500 is sufficient, there are enough adsorption sites for Cr(VI) and P(V), both Cr(VI) and P(V) can be fully removed. In other words, although P(V) influences the adsorption process of Cr(VI), when the concentration of CHTlc-500 is sufficient, both Cr(VI) and P(V) can be fully processed.

3.6. Materials recycling

Consideration of CHTlc-500 regeneration performance is important for this material to be used in practical applications. As CO_3^{2-} had strong affinity for CHTlc; thus, a solution of 10% $NaCO_3$ + 5% NaOH was selected for desorption. The results showed that the desorption solution was able to displace Cr(VI) and P(V) from CHTlc-500 laminates. After three desorption cycles, the P(V) desorption rate was no less than 80%, and that of Cr(VI) was no less than 90%. In addition, the desorbed CHTlc-500 could be reused by calcining at 500°C.

The regeneration was repeated four times, and the results are shown in Fig. 6. When CHTlc-500 was regenerated for the first time, the removal rates of P(V) and Cr(VI) were 100% and 99.64%, respectively. After three regeneration cycles, the adsorption capacity of CHTlc-500 did not change substantially. The removal rate of P(V) was 99.63% and the removal rate of Cr(VI) was 94.65%. This finding demonstrated CHTLc-500 was reusable and had good regeneration performance. In addition, the removal rate of P(V) was larger than that of Cr(VI) when adsorbed with regenerated CHTlc-500, which demonstrated that P(V) was more apt to occupy adsorption sites than Cr(VI).

When CHTlc-500 was regenerated for the fourth time, the removal rate of P(V) was 94.38%, but that of Cr(VI) dropped to 33.41%. Although CHTlc-500 can be regenerated, the incomplete desorption of Cr(VI) and P(V) due to the chemical adsorption of CHTlc-500 led to unremoved residual Cr(VI) and P(V) in the crystal. Unremoved Cr(VI) and P(V) still occupied some adsorption sites of the adsorbent after calcination at a high temperature. Besides, after several high-temperature calcinations, some CHTlc-500 was converted into spinel form ($MgAl_2O_4$) and led to the loss of adsorption capacity [58]. Generally, this good reusability and stability indicate the strong possibility of applying CHTlc-500 in Cr(VI) and P(V) treatment.

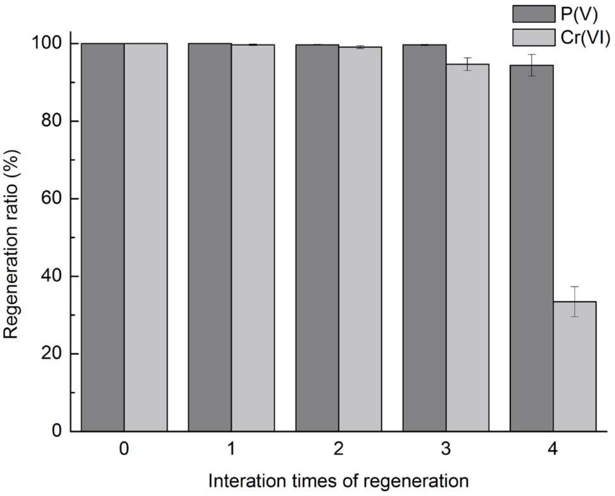

Fig. 6. Recoverability of CHTlc-500.

4. Conclusions

In this study, CHTlc-500 was synthesized and used as an adsorbent for the removal of Cr(VI) and P(V), CHTlc-500 showed good performance in adsorption. During the experimental process, the maximum adsorption occurs at 8 h and at a pH approximately 5. In competitive adsorption experiments, P(V) was more apt to be adsorbed on CHTlc-500 than Cr(VI). The existence of Cr(VI) did not significantly affected P(V) adsorption on CHTlc-500. When the concentration of Cr(VI) was 20 mg L^{-1}, the dosage of CHTlc-500 was 0.1 g, and P(V) concentration was below 10 mg L^{-1}, both Cr(VI) and P(V) could be removed at high removal rates. When the concentration of P(V) was in the range of 10 to 40 mg L^{-1}, P(V) obviously degraded Cr(VI) adsorption on CHTlc-500. The dosage of CHTlc-500 was important for the adsorption of Cr(VI) and P(V). When the amount of CHTlc-500 was inadequate, Cr(VI) and P(V) competed in the adsorption process and P(V) showed a stronger affinity to CHTlc-500. With the increase of CHTlc-500 dosage, the removal rate of both Cr(VI) and P(V) improved. In a mixture containing both Cr(VI) and P(V) at a concentration of 20 mg L^{-1}, when the adsorbent dosage was 1.0 g L^{-1}, Cr(VI) and P(V) could be completely removed. CHTlc-500 showed good regeneration performance during desorption in a solution of 10% $NaCO_3$ + 5% NaOH and calcining at 500°C. With an increase in regeneration time, the removal efficiency of CHTlc-500 decreased slightly but still remained high. After three regeneration cycles, the removal rates of P(V) and Cr(VI) were still 99.63% and 94.65%, which means the adsorbing material is effective and can be used more than once. The performance and reusability of CHTlc-500 indicate the potential for this material to be used in Cr(VI) and P(V) removal.

Acknowledgment

The authors are grateful for useful comments on the manuscript by Dr. Yulong Yan of Taiyuan University of Technology.

Symbols

q_t — Adsorption capacity at specific time t, mg g^{-1}
q_e — Equilibrium adsorption capacity, mg g^{-1}
R_t — Removal rate at specific time t, %
R_e — Equilibrium removal rate, %
C_0 — Initial Cr(VI) or P(V) concentration, mg L^{-1}
C_e — Equilibrium Cr(VI) or P(V) concentration, mg L^{-1}
C_t — Cr(VI) or P(V) concentration at specific time t, mg L^{-1}
V — Solution volume, L
W — Adsorbent mass, mg

References

[1] L. McNeill, J. McLean, M. Edwards, J. Parks, State of the Science of Hexavalent Chromium in Drinking Water, Water Research Foundation, Denver, CO, USA, 2012.
[2] P.K. Ghosh, Hexavalent chromium [Cr(VI)] removal by acid modified waste activated carbons, J. Hazard. Mater., 171 (2009) 116–122.
[3] D. Bregnbak, J.D. Johansen, M.S. Jellesen, C. Zachariae, T. Menné, J.P. Thyssen, Chromium allergy and dermatitis: prevalence and main findings, Contact Dermatitis, 73 (2015) 261–280.
[4] J. Guertin, C.P. Avakian, J.A. Jacobs, Chromium (VI) Handbook, CRC Press, Boca Raton, FL, USA, 2016.
[5] A. Zhitkovich, Chromium in drinking water: sources, metabolism, and cancer risks, Chem. Res. Toxicol., 24 (2011) 1617–1629.
[6] N. McCarroll, N. Keshava, J. Chen, G. Akerman, A. Kligerman, E. Rinde, An evaluation of the mode of action framework for mutagenic carcinogens case study II: chromium (VI), Environ. Mol. Mutagen., 51 (2010) 89–111.
[7] H. Klapper, Control of Eutrophication in Inland Waters, Ellis Horwood Ltd., Chichester, West Sussex, UK, 1991.
[8] J. Dai, H. Yang, H. Yan, Y.G. Shangguan, Q. Zheng, R.S. Cheng, Phosphate adsorption from aqueous solutions by disused adsorbents: chitosan hydrogel beads after the removal of copper (II), Chem. Eng. J., 166 (2011) 970–977.
[9] P.R.F. Bell, Eutrophication and coral reefs—some examples in the Great Barrier Reef lagoon, Water Res., 26 (1992) 553–568.
[10] I. Heidmann, W. Calmano, Removal of Cr(VI) from model wastewaters by electrocoagulation with Fe electrodes, Sep. Purif. Technol., 61 (2008) 15–21.
[11] S. Rayman, R.E. White, Simulation of reduction of Cr(VI) by Fe(II) produced electrochemically in a parallel-plate electrochemical reactor, J. Electrochem. Soc., 156 (2009) 96–104.
[12] L. Alidokht, A.R. Khataee, A. Reyhanitabar, S. Oustan, Reductive removal of Cr(VI) by starch-stabilized Fe^0 nanoparticles in aqueous solution, Desalination, 270 (2011) 105–110.
[13] G.-R. Xu, J.-N. Wang, C.-J. Li, Preparation of hierarchically nanofibrous membrane and its high adaptability in hexavalent chromium removal from water, Chem. Eng. J., 198 (2012) 310–317.
[14] A. Kaya, C. Onac, H.K. Alpoguz, A. Yilmaz, N. Atar, Removal of Cr(VI) through calixarene based polymer inclusion membrane from chrome plating bath water, Chem. Eng. J., 283 (2016) 141–149.
[15] T. Ölmez, The optimization of Cr(VI) reduction and removal by electrocoagulation using response surface methodology, J. Hazard. Mater., 162 (2009) 1371–1378.
[16] I. Heidmann, W. Calmano, Removal of Zn(II), Cu(II), Ni(II), Ag(I) and Cr(VI) present in aqueous solutions by aluminium electrocoagulation, J. Hazard. Mater., 152 (2008) 934–941.
[17] Y.Q. Xing, X.M. Chen, D.H. Wang, Electrically regenerated ion exchange for removal and recovery of Cr(VI) from wastewater, Environ. Sci. Technol., 41 (2007) 1439–1443.
[18] O. Kusku, B.L. Rivas, B.F. Urbano, M. Arda, N. Kabay, M. Bryjak, A comparative study of removal of Cr(VI) by ion exchange resins bearing quaternary ammonium groups, J. Chem. Technol. Biotechnol., 89 (2014) 851–857.
[19] N. Wang, Y.Z. Xu, L.H. Zhu, X.T. Shen, H.Q. Tang, Reconsideration to the deactivation of TiO$_2$ catalyst during simultaneous photocatalytic reduction of Cr(VI) and oxidation of salicylic acid, J. Photochem. Photobiol., A, 201 (2009) 121–127.
[20] J.Y. Yu, S.D. Zhuang, X.Y. Xu, W.C. Zhu, B. Feng, J.G. Hu, Photogenerated electron reservoir in hetero-p–n CuO–ZnO nanocomposite device for visible-light-driven photocatalytic reduction of aqueous Cr(VI), J. Mater. Chem. A, 3 (2015) 1199–1207.
[21] A. Baran, E. Bıçak, Ş.H. Baysal, S. Önal, Comparative studies on the adsorption of Cr(VI) ions on to various sorbents, Bioresour. Technol., 98 (2007) 661–665.
[22] A.K. Bhattacharya, T.K. Naiya, S.N. Mandal, S.K. Das, Adsorption, kinetics and equilibrium studies on removal of Cr(VI) from aqueous solutions using different low-cost adsorbents, Chem. Eng. J., 137 (2008) 529–541.
[23] G.H. Jing, Z.M. Zhou, L. Song, M.X. Dong, Ultrasound enhanced adsorption and desorption of chromium (VI) on activated carbon and polymeric resin, Desalination, 279 (2011) 423–427.
[24] J.H. Wang, X. Zhang, B. Zhang, Y.F. Zhao, R. Zhai, J.D. Liu, R.F. Chen, Rapid adsorption of Cr(VI) on modified halloysite nanotubes, Desalination, 259 (2010) 22–28.
[25] M. Gheju, I. Balcu, G. Mosoarca, Removal of Cr(VI) from aqueous solutions by adsorption on MnO$_2$, J. Hazard. Mater., 310 (2016) 270–277.
[26] Z.L. Ye, S.H. Chen, S.M. Wang, L.F. Lin, Y.J. Yan, Z.J. Zhang, J.S. Chen, Phosphorus recovery from synthetic swine wastewater by chemical precipitation using response surface methodology, J. Hazard. Mater., 176 (2010) 1083–1088.
[27] C. Aydiner, I. Demir, E. Yildiz, Modeling of flux decline in crossflow microfiltration using neural networks: the case of phosphate removal, J. Membr. Sci., 248 (2005) 53–62.
[28] G.L. Qiu, Y.M. Law, S. Das, Y.P. Ting, Direct and complete phosphorus recovery from municipal wastewater using a hybrid microfiltration-forward osmosis membrane bioreactor process with seawater brine as draw solution, Environ. Sci. Technol., 49 (2015) 6156–6163.
[29] N. Martí, L. Pastor, A. Bouzas, J. Ferrer, A. Seco, Phosphorus recovery by struvite crystallization in WWTPs: influence of the sludge treatment line operation, Water Res., 44 (2010) 2371–2379.
[30] W. Moerman, M. Carballa, A. Vandekerckhove, D. Derycke, W. Verstraete, Phosphate removal in agro-industry: pilot- and full-scale operational considerations of struvite crystallization, Water Res., 43 (2009) 1887–1892.
[31] M.L. Yu, D.Y. Yin, J. Shi, D.M. Song, Z.W. Xu, Phosphorus removal and recovery from high phosphorus wastewater by the HAP crystallization process, Orient. J. Chem., 32 (2016) 235–241.
[32] W.W. Huang, S.B. Wang, Z.H. Zhu, L. Li, X.D. Yao, V. Rudolph, F. Haghseresht, Phosphate removal from wastewater using red mud, J. Hazard. Mater., 158 (2008) 35–42.
[33] N.Y. Mezenner, A. Bensmaili, Kinetics and thermodynamic study of phosphate adsorption on iron hydroxide-eggshell waste, Chem. Eng. J., 147 (2009) 87–96.
[34] J.-W. Choi, S.-Y. Lee, S.-H. Lee, K.-B. Lee, D.-J. Kim, S.-W. Hong, Adsorption of phosphate by amino-functionalized and co-condensed SBA-15, Water Air Soil Pollut., 223 (2012) 2551–2562.

[35] J.B. Xiong, Y. Qin, E. Islam, M. Yue, W.F. Wang, Phosphate removal from solution using powdered freshwater mussel shells, Desalination, 276 (2011) 317–321.

[36] J. Lalley, C. Han, X. Li, D.D. Dionysiou, M.N. Nadagouda, Phosphate adsorption using modified iron oxide-based sorbents in lake water: kinetics, equilibrium, and column tests, Chem. Eng. J., 284 (2016) 1386–1396.

[37] G.R. Qian, L.L. Feng, J.Z. Zhou, Y.F. Xu, J.Y. Liu, J. Zhang, Z.P. Xu, Solubility product (Ksp)-controlled removal of chromate and phosphate by hydrocalumite, Chem. Eng. J., 181 (2012) 251–258.

[38] Ş. Ertul, M. Bayrakcı, M. Yilmaz, Removal of chromate and phosphate anion from aqueous solutions using calix[4]aren receptors containing proton switchable units, J. Hazard. Mater., 181 (2010) 1059–1065.

[39] S. Mandal, S. Mayadevi, Adsorption of fluoride ions by Zn–Al layered double hydroxides, Appl. Clay Sci., 40 (2008) 54–62.

[40] S.-L. Wang, C.H. Liu, M.K. Wang, Y.H. Chuang, P.N. Chiang, Arsenate adsorption by Mg/Al–NO_3 layered double hydroxides with varying the Mg/Al ratio, Appl. Clay Sci., 43 (2009) 79–85.

[41] L. Lv, J. He, M. Wei, D.G. Evans, Z.L. Zhou, Treatment of high fluoride concentration water by MgAl-CO_3 layered double hydroxides: kinetic and equilibrium studies, Water Res., 41 (2007) 1534–1542.

[42] K.D. Collins, M.W. Washabaugh, The Hofmeister effect and the behavior of water at interfaces, Q. Rev. Biophys., 18 (1985) 323–422.

[43] T. Sato, S. Onai, T. Yoshioka, A. Okuwaki, Causticization of sodium carbonate with rock-salt type magnesium aluminium oxide formed by the thermal decomposition of hydrotalcite-like layered double hydroxide, J. Chem. Technol. Biotechnol., 57 (1993) 137–140.

[44] P. Cai, H. Zheng, C. Wang, H.W. Ma, J.C. Hu, Y.B. Pu, P. Liang, Competitive adsorption characteristics of fluoride and phosphate on calcined Mg–Al–CO_3 layered double hydroxides, J. Hazard. Mater., 213 (2012) 100–108.

[45] H.T. Zhu, Y.J. Ma, Progress in application of hydrotalcite-like materials in heavy metal wastewater treatment, Technol. Water Treat., 37 (2011) 11–14.

[46] J.L. Sun, W.J. Zhen, J. Li, Structure, properties and applications of LDHs, Chem. Ind. Eng. Prog., 32 (2013) 610–616.

[47] L. Lv, J. He, M. Wei, D.G. Evans, X. Duan, Factors influencing the removal of fluoride from aqueous solution by calcined Mg–Al–CO_3 layered double hydroxides, J. Hazard. Mater., 133 (2006) 119–128.

[48] X.L. Song, Y.H. Wu, Simultaneous adsorption of chromium (VI) and phosphate by calcined Mg-Al-CO_3 layered double hydroxides, Bull. Korean Chem. Soc., 35 (2014) 1817–1824.

[49] J.S. Wu, Y.K. Xiao, J.Y. Wan, L.R. Wen, The growth mechanism of hydrotalcite crystal, Sci. China Technol. Sci., 55 (2012) 872–878.

[50] Y.Q. Yang, N.Y. Gao, W.H. Chu, Y.J. Zhang, Y. Ma, Adsorption of perchlorate from aqueous solution by the calcination product of Mg/(Al–Fe) hydrotalcite-like compounds, J. Hazard. Mater., 209 (2012) 318–325.

[51] Y. Li, L.W. Shi, Z.S. Liu, G.Q. Yang, Sorption of o-cresol on pristine, calcined and modified hydrotalcite-like compounds, Acta Chim. Sinica, 70 (2012) 683–690.

[52] X.-H. Wang, F.-F. Liu, L. Lu, S. Yang, Y. Zhao, L.-B. Sun, S.-G. Wang, Individual and competitive adsorption of Cr(VI) and phosphate onto synthetic Fe–Al hydroxides, Colloids Surf., A, 423 (2013) 42–49.

[53] D.J. Kang, X.L. Yu, S.R. Tong, M.F. Ge, J.C. Zuo, C.Y. Cao, W.G. Song, Performance and mechanism of Mg/Fe layered double hydroxides for fluoride and arsenate removal from aqueous solution, Chem. Eng. J., 228 (2013) 731–740.

[54] X. Cheng, X.R. Huang, X.Z. Wang, D.Z. Sun, Phosphate adsorption by ZnAlLa layered double hydroxides from excess sludge filtrate, CIESC J., 61 (2010) 955–962.

[55] M.X. Zhu, Y.P. Li, L. Zhang, H.W. Ji, Adsorption of phosphate by hydrotalcite and its calcined product, Acta Miner. Sinica, 25 (2005) 27–32.

[56] Y. Ye, S.J. Yang, L.B. Zheng, Z.Y. Shen, S.S. Ji, X. Huang, Comparison and discussion on the adsorption capacity of several compounds with layered structure, J. Inorg. Mater., 19 (2004) 1379–1385.

[57] G.-X. Pan, P.-P. Qian, F. Cao, Z.-M. Ni, Thermal stability and ion-exchange properties of layered double hydroxides investigation based on the second law of crystal chemistry, Acta Miner. Sinica, 33 (2013) 25–30.

[58] W.D. Wang, R.X. Hao, X.X. Zhu, J.J. Wan, L.Y. Zhong, Regeneration method and mechanism of phosphorus adsorbent Mg/Al-LDO, China Environ. Sci., 37 (2017) 2092–2099.